Quantitative surface stress measurements using a microcantilever

Michel Godin,[a] Vincent Tabard-Cossa, and Peter Grütter
Department of Physics, McGill University, 3600 University Street, Montréal, Québec, H3A 2T8 Canada

Peter Williams
Department of Physics, Acadia University, Wolfville, Nova Scotia, B0P 1X0, Canada

(Received 23 April 2001; accepted for publication 31 May 2001)

A method for calculating the surface stress associated with the deflection of a micromechanical cantilever is presented. This method overcomes some of the limitations associated with Stoney's formula by circumventing the need to know the cantilever's Young's modulus, which can have a high level of uncertainty, especially for silicon nitride cantilevers. The surface stress is calculated using readily measurable cantilever properties, such as its geometry, spring constant, and deflection. The method is applicable to both rectangular and triangular cantilevers. A calibration of the deflection measurement is also presented. The surface stress measurement is accurate to within 4%–7%. © *2001 American Institute of Physics.* [DOI: 10.1063/1.1387262]

The atomic-force microscope (AFM) cantilever has proven to be indispensable in many surface science applications. Not only is it of crucial importance in scanning probe microscopes, but AFM micromachined cantilevers are an important component in many micromechanical sensors. Their small size results in very sensitive and fast measurements. Recent experiments have used AFM cantilevers as versatile sensors to distinguish between oligonucleotide (DNA) molecules of different base sequences,[1] to detect single biomolecules,[2] to measure *p*H changes,[3] and to measure the surface stress associated with molecular adsorption[4,5] or absorption.[6,7] In many of these applications, the deflection of the cantilever is driven by the build up of surface stress as its surface is modified. Having a method to quantify this surface stress with respect to the cantilever's deflection is very important.

The surface stress associated with the deflection of an AFM cantilever is commonly calculated using Stoney's formula,[8] which simply relates an induced substrate curvature to a surface stress. Unfortunately, calculating the surface stress using Stoney's formula requires Young's modulus E of the cantilever material to be known. This is problematic in the case of commonly used SiN_x AFM cantilevers, where the uncertainty in E is very high ($E \approx 130-385$ GPa),[9,10] since the exact atomic ratio between Si and N is not determined.[9] Furthermore, the addition of metallic or polymeric coatings on the cantilever surface can significantly modify the cantilever's elastic properties.[10] Although recent articles[11–13] have made improvements on Stoney's approach, they still require knowledge of Young's modulus, which introduces large uncertainty in the calculated surface stress.

We derive below an alternate relation to Stoney's formula relating the induced cantilever deflection to the corresponding surface stress, which only requires the knowledge of the geometry, spring constant, and Poisson's ratio of the cantilever. Using a measured spring constant completely eliminates the need to evaluate the resulting Young's modulus of the metal-coated cantilever. This relation is based on calculating the energy stored in the stressed cantilever, while assuming that its deflection is entirely due to a surface stress.

The energy stored in a bent cantilever can be calculated from its spring constant k and the deflection at its apex, Δz, using Hooke's law. However, the spring constant associated with an AFM cantilever is usually used to relate a deflection to a force which is applied as a concentrated load at the apex (tip) of the cantilever. In the case of a molecular adsorption-induced surface stress, we must account for the fact that the cantilever deflection is the result of an isotropic surface stress, which acts over the entire surface of the cantilever. The energy stored in a stressed cantilever, E_k, can be written from a modified Hooke's law as

$$E_k = \left(\frac{4}{3(1-\nu)}\right)\frac{1}{2}k\Delta z^2, \tag{1}$$

where the factor **4/3** takes into account the different cantilever beam curvatures resulting from a uniform surface stress, as opposed to a concentrated load applied at the tip. This factor can be derived by comparing the strain energies of a cantilever that is deflected by a concentrated load and one deflected by a surface stress.[9,14,15] In Eq. (1), k refers to the spring constant associated with a typical AFM experiment, where a concentrated load at the tip is applied to the cantilever. k needs to be replaced by $k/(1-\nu)$, where ν is the cantilever's Poisson's ratio, since the surface stress acting on the cantilever surface is isotropic.[9,12]

The energy stored in a stressed cantilever[15] can also be calculated from

$$E_{\text{elastic}} = \int_0^l \frac{M^2}{2E^*I}dy, \tag{2}$$

where M is the bending moment of the cantilever beam; E^* is its biaxial modulus,[9,12] which is related to its Young modulus E as $E^* = E/(1-\nu)$; I is the area moment of inertia; and the integration is carried over the length of the cantilever, l. We are able to substitute the elastic constants E^* and I with the radius of curvature R using the general differential equation for an elastic beam[15]

$$\frac{d^2z}{dy^2} \cong \frac{1}{R} = \frac{M}{E^*I}. \tag{3}$$

[a]Electronic mail: mgodin@physics.mcgill.ca

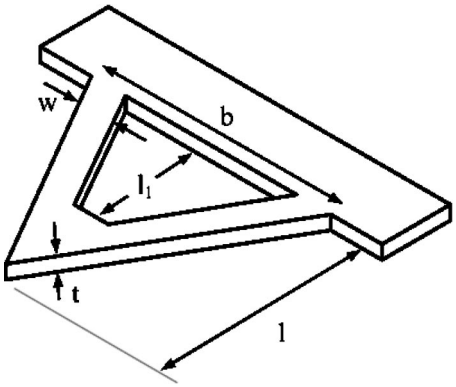

FIG. 1. Triangular cantilever geometry. For a rectangular cantilever, W is the leg width.

We can write the bending moment M, denoted by M_{rect} and M_{Δ} for rectangular and triangular cantilevers, respectively, as[16]

$$M_{\text{rect}}=\frac{\Delta\sigma W t}{2}, \tag{4}$$

$$M_{\Delta}=\begin{cases}\Delta\sigma W t & \text{for } 0\leqslant y\leqslant l_1,\\ \dfrac{\Delta\sigma t b(l-y)}{2l} & \text{for } l_1<y\leqslant l,\end{cases} \tag{5}$$

where W, t, l, l_1, and b are depicted in Fig. 1, and $\Delta\sigma$ is the difference in surface stress between the top and bottom surfaces of the cantilever.

Although the cantilever does not bend circularly when exposed to an isotropic surface stress, we found its radius of curvature is to a good approximation constant over its length, as long as the deflection Δz is much smaller than the overall length of the cantilever. This is true for typical surface stress measurements. The radius of curvature can then be expressed as

$$R\approx\frac{l^2}{2\Delta z}. \tag{6}$$

Finally, by inserting Eq. (3) into Eq. (2), and by then substituting M and R by Eq. (4) (for rectangular cantilevers), or Eq. (5) (for triangular cantilevers), and Eq. (6), the integration can be performed over the length of the cantilever to obtain the strain energy stored in the stressed cantilever. By equating this resulting strain energy to the energy calculated using the modified Hooke's law stated in Eq. (1), the differential surface stress acting on a rectangular cantilever becomes

$$\Delta\sigma=\frac{4}{3(1-\nu)}\frac{l}{Wt}k_{\text{rect}}\Delta z, \tag{7}$$

and on a triangular cantilever,

$$\Delta\sigma=\frac{2}{3(1-\nu)}\frac{l^2}{\left[Wtl_1+\dfrac{tb}{4l}(l-l_1)^2\right]}k_{\Delta}\Delta z, \tag{8}$$

where k_{rect} and k_{Δ} are the spring constants for rectangular and triangular cantilevers, respectively. The geometrical parameters W, l, l_1, and b can all be measured using a calibrated optical microscope or a scanning electron microscope (SEM). The cantilever thickness t can be measured using a calibrated AFM, a precise SEM, or deduced from a measurement of the rectangular cantilever's spring constant.[14,17] k_{rect} can be easily evaluated from its resonant frequency and quality factor measured in a fluid (e.g., air).[17] In the case where the triangular cantilever is mounted on the same chip as a rectangular cantilever,[18] its spring constant, k_{Δ}, can be determined from geometrical parameters and from the rectangular cantilever's spring constant, k_{rect}, as pointed out by Sader and co-workers.[17,19] Finally, the cantilever deflection Δz is measured using an optical beam deflection technique, the calibration of which will be described below.

Using the above formalism, we can measure the surface stress with an accuracy and a repeatability of approximately 4%–7%. We took Poisson's ratio to be equal to 0.25 since both SiN_x and the Au coating are isotropic materials.[20] However, the uncertainty in Poisson's ratio was the major contributor to error in the calculation of surface stress. Poisson's ratio for SiN_x has been quoted as ranging from 0.2 to 0.3,[9] which translates into a maximum uncertainty of 7% in the surface stress, as calculated using Eq. (7). A less conservative estimate for Poisson's ratio is 0.25 ± 0.02, which includes most values as stated in the literature.[9,10,19,21,22] This yields a typical uncertainty in the surface stress of 4%. We found the variability in the measured spring constants from cantilever to cantilever taken randomly from the same wafer to be of the order of 2%. Consequently, we found it reasonable to make a spring constant measurement on a single cantilever and assume this to be uniform over the entire wafer. The cantilever thickness was measured with an uncertainty of approximately 1.4%. The cantilever deflection was measured with an accuracy better than 1%, as described below. The remaining geometrical parameters were measured with negligible uncertainties.

In most cantilever-based chemical sensors, Δz is monitored using an optical beam deflection technique, where a laser beam is focused onto the apex of the cantilever, and the reflected beam is detected by a position-sensing (photo)detector (PSD). In order to relate the PSD signal to the cantilever deflection, we induce a deflection and measure the PSD signal. Simultaneously, we directly measure the deflection with a fiber-optic interferometer,[23] which is positioned at the end of the cantilever from the opposite side. For small deflections, the PSD signal ΔS is proportional to the deflection of the cantilever, Δz,

$$\Delta z=C_{\text{cal}}\Delta S, \tag{9}$$

where C_{cal} is the calibration constant to be determined. The output of the interferometer is given by

$$V_{\text{int}}=A\sin\left(\frac{4\pi}{\lambda}\Delta z+\phi\right)+B, \tag{10}$$

where A and B are constants, ϕ is a phase angle, and λ is the interferometer laser wavelength. Substituting Eq. (9) into Eq. (10), we get

$$V_{\text{int}}=A\sin\left(\frac{4\pi}{\lambda}C_{\text{cal}}\Delta S+\phi\right)+B. \tag{11}$$

If we determine the frequency K_{int}, from a plot of the interferometer signal versus the PSD signal, C_{cal} can be found from

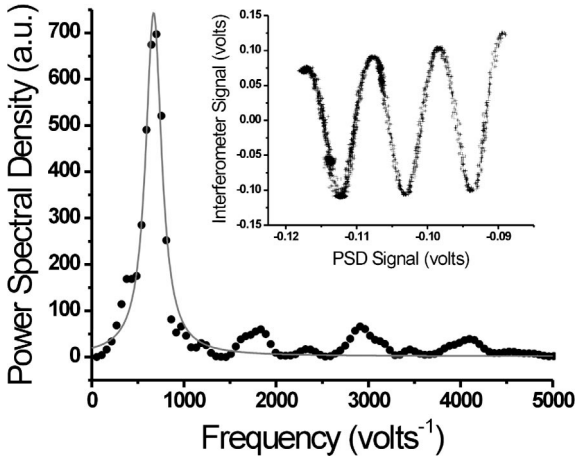

FIG. 2. Data from a typical calibration run. The slope observable in the interferometer signal (inset) is due to its intensity varying as the distance from the fiber end to the cantilever changes. The power spectral density for these data is shown with a Lorentzian fit. From the fit, we find $K_{\mathrm{int}}=671 \pm 1\ \mathrm{V}^{-1}$.

$$C_{\mathrm{cal}}=\frac{K_{\mathrm{int}}\lambda}{4\pi}. \tag{12}$$

Experimentally, approximately 6 mA is passed through a 1.5 kΩ surface mount resistor placed in good thermal contact with the chip of the gold-coated cantilever. After 10 s, the power supply is turned off and data are collected during cooling. The custom-built fiber-optic interferometer operating at 635 nm is positioned behind the apex of the cantilever using an $x-y$ positioning stage. We assure that the fiber is as high on the apex as possible by sweeping the fiber from side to side with a micrometer screw, while noting the positions at which the interferometer signal vanishes. The fiber is then repositioned half way in between these two positions and moved up until the interferometer signal just starts to vanish. This procedure results in the fiber being reproducibly positioned at the tip of the cantilever. The actual position of the interferometer fiber can be estimated knowing the fiber's numerical aperture and the distance between its cleaved end and the cantilever surface, which is approximately equal to half the fiber's outer diameter of 80 μm. In our case, we found the interferometer fiber to be positioned approximately 8 μm from the end of the cantilever. This distance, Δl, indicates the actual position at which the cantilever deflection is measured. Because we require the deflection of the apex of the cantilever in Eqs. (7) and (8), we correct the Δz measured in this way by a factor of $l^2/(l-\Delta l)^2$. A typical data set is shown in the inset of Fig. 2.

To extract K_{int} from these data, we used the Lomb[24] technique for spectral estimation with unevenly sampled data. Figure 2 shows the power spectral density calculated for that data, with a Lorentzian fit. From the fit, we find the peak center at $671\pm 1\ \mathrm{V}^{-1}$. Thus, for a single run, we find $C_{\mathrm{cal}}=(3.391\pm 0.005)\times 10^{-5}\ \mathrm{m\,V}^{-1}$. We found this procedure to yield cantilever deflection measurements that are accurate and reproducible to within 1%. We also found that this uncertainty is not increased when refocusing the laser beam used for the beam deflection setup and repositioning the cantilever chip, as is normally done between successive experiments. The laser beam is reproducibly focused on the cantilever apex by maximizing the total signal into the PSD.

AFM cantilevers are increasingly being used as a platform to measure the surface stress associated with molecular adsorption. We have shown in this letter a method to calculate the surface stress from the cantilever deflection using readily measurable cantilever properties, such as its geometry, spring constant, and Poisson's ratio. It is an attractive alternative to using Stoney's formula since it circumvents the need to know Young's modulus for the cantilever, which often carries a high level of uncertainty. Finally, we have shown a method for calibrating the deflection measurement by relating the optical beam deflection measurement to a direct measure of the deflection obtained using a fiber interferometer. These procedures allow us to reproducibly and accurately determine the surface stress associated with the deflection of a cantilever to better than 4%.

The authors would like to thank B. Hunt for his spring constant measurements and A. Mitchell for many helpful discussions. This work was supported by the Natural Sciences and Engineering Reasearch Council of Canada (NSERC).

[1] J. Fritz, M. K. Baller, H. P. Lang, H. Rothuizen, P. Vettiger, E. Meyer, H.-J. Güntherodt, Ch. Gerber, and J. K. Gimzewski, Science **288**, 316 (2000).
[2] B. Illic, D. Czaplewski, H. G. Craighead, P. Neuzil, C. Campagnolo, and C. Batt, Appl. Phys. Lett. **77**, 450 (2000).
[3] J. Fritz, M. K. Baller, H. P. Lang, T. Strunz, E. Meyer, H.-J. Güntherodt, E. Delamarche, Ch. Gerber, and J. K. Gimzewski, Langmuir **16**, 9694 (2000).
[4] R. Berger, E. Delamarche, H. P. Lang, Ch. Gerber, J. K. Gimzewski, E. Meyer, and H.-J. Güntherodt, Science **276**, 2021 (1997).
[5] T. Thundat, E. A. Wachter, S. L. Sharp, and R. J. Warmack, Appl. Phys. Lett. **66**, 1695 (1995).
[6] H. Jensenius, J. Thaysen, A. A. Rasmussen, L. H. Veje, O. Hansen, and A. Boisen, Appl. Phys. Lett. **76**, 2615 (2000).
[7] M. K. Baller, H. P. Lang, J. Fritz, Ch. Gerber, J. K. Gimzewski, U. Drechsler, H. Rothuizen, M. Despont, P. Vettiger, F. M. Battiston, J. P. Ramseyer, P. Fornaro, E. Meyer, and H.-J. Güntherodt, Ultramicroscopy **82**, 1 (2000).
[8] G. G. Stoney, Proc. R. Soc. London, Ser. A **82**, 172 (1909).
[9] T. Miyatani and M. Fujihira, J. Appl. Phys. **81**, 7099 (1997).
[10] J. E. Sader, I. Larson, P. Mulvaney, and L. R. White, Rev. Sci. Instrum. **66**, 3789 (1995).
[11] J. E. Sader, J. Appl. Phys. **89**, 2911 (2001).
[12] L. B. Freund, J. A. Floro, and E. Chason, Appl. Phys. Lett. **74**, 1987 (1999).
[13] Cl. A. Klein, J. Appl. Phys. **88**, 5487 (2000).
[14] M. Godin, M.Sc. thesis, McGill University (2000).
[15] D. Sarid, *Scanning Force Microscopy with Applications to Electric, Magnetic and Atomic Forces* (Oxford University Press, New York, 1994), Chap. 1.
[16] G. Y. Chen, T. Thundat, E. A. Wachter, and R. J. Warmack, J. Appl. Phys. **77**, 3618 (1995).
[17] J. E. Sader, J. W. M. Chon, and P. Mulvaney, Rev. Sci. Instrum. **70**, 3967 (1999).
[18] Thermomicroscopes, 1171 Borregas Ave., Sunnyvale, CA 94089.
[19] J. E. Sader, Rev. Sci. Instrum. **66**, 4583 (1995).
[20] S. Timoshenko and D. H. Young, *Elements of Strength of Materials*, 4th ed. (Van Nostrand, New York, 1962), Chap. 1, p. 11.
[21] R. Berger, E. Delamarche, H. P. Lang, Ch. Gerber, J. K. Gimzewski, E. Meyer, and H.-J. Güntherodt, Appl. Phys. A: Mater. Sci. Process. **66**, S55 (1998).
[22] J. M. Neumeister and W. A. Ducker, Rev. Sci. Instrum. **65**, 2527 (1994).
[23] D. Rugar, H. J. Mamin, and P. Güthner, Appl. Phys. Lett. **55**, 2588 (1989).
[24] W. H. Press, S. A. Teukolsky, W. T. Vetterling, and B. P. Flannery, *Numerical Recipes in C: The Art of Scientific Computing*, 2nd ed. (Cambridge University Press, New York, 1997), Chap. 13.8, p. 575.